

Malaysian Congress of Radiology (MCOR) 2018

Malaysian Society of Interventional Radiology (MYSIR) 2018

in conjunction with

13th Asian-Australasian Federation of Interventional & Therapeutic Neuroradiology (AAFITN) 2018

7th-9th March 2018

Venue: The Magellan Sutera Hotel & Convention Centre, Kota Kinabalu, Sabah, Malaysia
www.aafitn2018malaysia.com



CONTENTS

- S2 **Welcome Message from the Organising Chairman and President of the MYSIR**
- S3 **Welcome Message from the President of the College of Radiology, Academy of Medicine of Malaysia**
- S4 **Summary of Abstracts**
- S6 **Abstracts: MCOR 2018: Body Imaging**
- S13 **Abstracts: MCOR 2018: Breast Radiology**
- S15 **Abstracts: MCOR 2018: Musculoskeletal**
- S20 **Abstracts: MCOR 2018: Neuroradiology**
- S23 **Abstracts: MCOR 2018: Paediatric Radiology**
- S25 **Abstracts: MYSIR 2018: Interventional Radiology (Non-neurological)**

CONFERENCE SECRETARIAT

MCOR and MYSIR Secretariat
Email: secretariat@aafitn2018malaysia.com

ORGANISER

College of Radiology, Academy of Medicine of Malaysia
Unit 2.4 (Suite 1), Enterprise 3B, Jalan Innovasi 1
Technology Park Malaysia
Lebuhraya Puchong-Sungei Besi
57000 Bukit Jalil, Kuala Lumpur, Malaysia
Email: secretariat@radiologymalaysia.org

Malaysian Society of Interventional Radiology
Unit 2.4 (Suite 1), Enterprise 3B, Jalan Innovasi 1
Technology Park Malaysia
Lebuhraya Puchong-Sungei Besi
57000 Bukit Jalil, Kuala Lumpur, Malaysia
Email: secretariat@mysir.org

Welcome Message



From the Organising Chairman and President of the MYSIR

This year, the Malaysian Congress of Radiology (MCOR) 2018 and the Malaysian Society of Interventional Radiology (MYSIR) 2018 are held in conjunction with the 13th Asian-Australasian Federation of Interventional and Therapeutic Neuroradiology in Kota Kinabalu, Sabah, Malaysia, from 7–9 March 2018.

The theme of this year's meetings is 'Strengthening Foundations and Exploring New Concepts'. We are inordinately pleased that the free papers submitted for oral and poster presentations reflect this theme. We received 111 free papers for the MCOR 2018 and the MYSIR 2018. These papers comprised studies done by our local researchers and those from countries such as Australia, China, Korea and the Philippines. In an effort to encourage more submissions of oral presentations among our members and colleagues, a number of quality abstracts that were submitted for poster presentations were given the opportunity to be published in the *Singapore Medical Journal*. This supplement issue showcases the highest scoring abstracts submitted for this year's meetings.

I would like to thank the Scientific Chairmen, Dr Naveen Rajadurai of the MCOR and Dr Norshazriman Sulaiman of the MYSIR, and their respective Scientific Committees, for rising to the occasion of organising this year's MCOR and MYSIR meetings. I am sure our participants, especially the younger radiologists, will enjoy the sessions that have been lined up.

We look forward to meeting and learning from all of you in these next three days. On behalf of my committee, I wish you 'selamat datang – welcome to Kota Kinabalu.



Dr Jeyaledchumy Mahadevan

Organising Chairman,

13th Asian-Australasian Federation of Interventional and Therapeutic Neuroradiology

Welcome Message



From the President of the College of Radiology, Academy of Medicine of Malaysia

The College of Radiology, Academy of Medicine of Malaysia is honoured to be a part of the 13th Asian-Australasian Federation of Interventional and Therapeutic Neuroradiology, which is being held for the first time in Malaysia along with the 2018 Malaysian Society of Interventional Radiology annual scientific meeting.

The College of Radiology, Academy of Medicine of Malaysia is also deeply honoured to have abstracts submitted for the Malaysian Congress of Radiology (MCOR) 2018 published in the prestigious *Singapore Medical Journal*. For this meeting, we received submissions from various disciplines, namely neuroradiology, body imaging, breast imaging, molecular imaging/nuclear medicine, musculoskeletal radiology and paediatric radiology.

The MCOR 2018 will focus on back-to-basics and updates in the fields of thoracic radiology, breast radiology and musculoskeletal radiology. There are also special sessions for radiographers/radiologic technologists lined up in our programme. This meeting will be an occasion for radiologists from around the world to meet, make friends, renew friendships and exchange ideas about their knowledge and practice in this fascinating specialty of medicine we love – radiology.

We sincerely hope that besides enjoying the scientific programme of this congress, you will take some time to sightsee around the beautiful city of Kota Kinabalu. On behalf of the College of Radiology, Academy of Medicine of Malaysia and the organising committee, I would like to wish everyone a warm 'selamat datang' to this meeting.

A handwritten signature in black ink, reading 'Amir Fuad Hussain'.

Dr Amir Fuad Hussain
President (2016–2018)
College of Radiology
Academy of Medicine of Malaysia

Abstract No.	Title	Presenter
Category: MCOR 2018: Body Imaging		
BD001	Quantification of apparent diffusion coefficient values to differentiate hepatocellular carcinoma and liver haemangioma in diffusion-weighted magnetic resonance imaging	Andrew Cheng
BD002	Tongue cavernous haemangioma	Hairuddin Achmad Sankala
BD003	Hughes-Stovin syndrome: a case report	Isa Azzaki Zainal
BD004	Troubleshooting the implementation of dual-energy computed tomography pulmonary angiography for the diagnosis of pulmonary emboli at a large level 1 trauma centre	James Ling
BD005	The effect of a modified alternate-day calorie restriction programme on nonalcoholic fatty liver disease	Khairiah Mat Yusoff
BD006	Undescended testes: not the end of story, but the beginning	Khor Foo Kiang
BD007	Focal chronic pyelonephritis mimicking renal cell carcinoma: a case report	Manju T Raja
BD008	A cross-sectional study to assess the agreement between Doppler ultrasonography and nonenhanced magnetic resonance angiography in diagnosing significant main renal artery stenosis and its influencing factors	Mazeda Murad
BD009	Vanek's tumour causing ileoileal intussusception in an adult lady: a case report	Norain Talib
BD010	The association of findings from thoracic computed tomography with galactomannan and <i>Aspergillus</i> -specific polymerase chain reaction for the diagnosis of invasive aspergillosis in patients with febrile neutropenia	Juhara Haron
BD011	Pancreatic head mass: now you see it, now you don't	Phyllis Wan Chun Ho
BD012	Erosive juvenile polyarticular tophaceous gout with hyoid bone involvement	Teik Beng Chuah
BD013	Measurement of middle-ear volume in adults using three-dimensional reconstruction multidetector computed tomography	Siti Khairunnisaak Abdul Rahman
BD014	A comparison of the HepaFat-scan® and the FibroScan® with controlled attenuation parameter in the estimation of hepatic steatosis in patients with nonalcoholic fatty liver disease using histology as the reference standard	Syaman Harry
BD015	A rare case of biopsied proven renal synovial sarcoma in a young adult patient: a case report and literature review	Wong Sheau Ning
Abstract No.	Title	Presenter
Category: MCOR 2018: Breast Radiology		
BR001	The spectrum of papillary breast lesions in the Malaysia population: radiopathological considerations	Farhana Fadzli
BR002	Diagnostic accuracy and clinical feasibility of vacuum-assisted breast biopsy of non-palpable breast lesions: a single-centre experience	Kartini Rahmat
BR003	The usefulness and diagnostic accuracy of tomosynthesis in characterising mammographic abnormality	Marlina Tanty Ramli
BR004	The impact of multimodality imaging on clinical decision-making in breast cancer patients selected for intraoperative radiotherapy	Wai Yee Chan
Abstract No.	Title	Presenter
Category: MCOR 2018: Musculoskeletal		
MS001	The unique 'dot-in-circle' sign on magnetic resonance imaging in a case of Madura foot	Apsara Panicker
MS002	Multiple enchondromatosis (Ollier disease): a rare case in the Philippines	Ernie Bautista II
MS003	An uncommon presentation of a giant cell tumour	Alex Fook Seng Lee
MS004	A correlation between ultrasonographic dynamic evaluation and clinical laxity grading of anterior talofibular ligament and calcaneofibular ligament tears among athletes	Indar Rahini Hairi
MS005	A case of osteogenesis imperfecta	Jerik Yumol
MS006	Multidetector computed tomography arthrography of the shoulder is a better cost-saving imaging modality in suburban hospitals: a pictorial essay	Ming Huan Cheng
MS007	Thrower's fracture: a rare injury from a rare sport in Malaysia	Mohd Shukry Mohd Khalid
MS008	Cadaveric stature estimation in the Malaysian population using postmortem computed tomography	Sabrilhakim Sidek
MS009	Morphologic changes of the rotator cuff muscles following fast isokinetic training in state-level weightlifters	Siti Salwa Mohamad Zaini

Abstract No.	Title	Presenter
Category: MCOR 2018: Neuroradiology		
NR001	Neuroimaging abnormalities in anti-NMDA receptor encephalitis	Alan Basil Peter
NR002	Computed tomography and magnetic resonance imaging of the brain in MELAS syndrome: a case report	Andrew Cheng
NR004	Regional diffusion tensor imaging-derived tensor metrics from white matter tracts for the characterisation of gliomas	Pohchoo Seow
NR005	Malignant melanoma of the nasal cavity	Rofiah Ali
NR006	Microstructural integrity of the peripheral nerves in Charcot-Marie-Tooth disease: a magnetic resonance imaging evaluation study	Thiagu Krisnan
NR007	Vein of Galen aneurysmal malformation: a case of an uncommon intracranial vascular malformation and literature review	Yeong Huei Yiauw
NR008	A rare case of tectal plate glioma with a typical presentation of obstructive hydrocephalus	Yuh Yang Leong
Abstract No.	Title	Presenter
Category: MCOR 2018: Paediatric Radiology		
PD001	Establishing the reference value for normal liver stiffness among healthy children assessed by point shear wave elastography imaging	Kuan Siong Sim
PD002	Orbital manifestations of Langerhans cell histiocytosis: a case report	Nur Asma Sapiai
PD003	Biliary rhabdomyosarcoma: a diagnostic challenge	See Khim Sim
Abstract No.	Title	Presenter
Category: MYSIR 2018: Interventional Radiology (Non-neurological)		
MY001	The correlation between arteriovenous fistula stenosis and haemodialysis parameters before and after angioplasty	Ani Darwina Abd Halim
MY002	Extended endovenous laser therapy of the long saphenous vein: a safe procedure that reduces the need for additional sclerotherapy	Eric Chung
MY004	Selective hepatic arterial embolisation of the hepatic arteriobiliary fistula secondary to lupus vasculitis	Kia Sing Tan
MY005	Selective salpingography and fallopian tube recanalisation: the University Malaya Medical Centre experience	Anushya Vijayanathan
MY006	Common iliac vein stenting for the treatment of chronic lower limb swelling due to preferential drainage of the lower limb vein into the pelvic arteriovenous malformation	Mohd Naim Mohd Yaakob
MY007	Prostatic artery embolisation for acute urinary retention secondary to benign prostate hyperplasia	Mohd Naim Mohd Yaakob
MY008	A comparison of cone beam computed tomography with multislice computed tomography in the identification of common periprocedural intracranial pathologies	Izzatul Aini Mohamad Idris
MY009	Comparing central line-associated bloodstream infection rate between tunnelled and cuffed peripherally inserted central catheters	Sze Yong Teoh

CATEGORY: MCOR 2018: BODY IMAGING

BD001

Quantification of apparent diffusion coefficient values to differentiate hepatocellular carcinoma and liver haemangioma in diffusion-weighted magnetic resonance imaging

Andrew Cheng¹, Yan Lin Li¹, Shirley Ho¹, Mabel Tong²

¹Radiology, Queen Mary Hospital, ²Radiology, North District Hospital, Hong Kong

INTRODUCTION Differentiation of liver lesions remains difficult in magnetic resonance (MR) imaging studies. Quantification of apparent diffusion coefficient (ADC) values using diffusion-weighted MR imaging (DWI) can help to characterise liver lesions. The purpose of this study was to evaluate the diagnostic value of ADC quantification in differentiating hepatocellular carcinoma (HCC) and liver haemangioma.

METHODS We retrospectively studied 35 patients in whom DWI/ADC studies were performed in Queen Mary Hospital, Hong Kong, from January 2014 to October 2017. HCC was diagnosed either by hepatectomy or intraoperative exploration. Liver haemangioma was diagnosed by the classical signs of progressive contrast filling in enhancement pattern. ADC values were calculated from DWI images with b-values at 50, 400 and 800 s/mm² (Siemens) and b-values at 0 and 300 s/mm² (General Electric Medical Systems). ADC values of HCC and

liver haemangioma were compared using two-tailed Mann-Whitney *U* test. A statistically significant difference was set at p-value < 0.05.

RESULTS 14 and 21 patients were diagnosed with HCC and liver haemangioma, respectively. Mean ADC value of patients diagnosed with HCC and liver haemangioma was $1.0363 \pm 0.3382 \times 10^{-3}$ mm²/s and $2.6243 \pm 0.7517 \times 10^{-3}$ mm²/s, respectively. ADC values were significantly lower in HCC patients than in liver haemangioma patients (*p* < 0.05).

CONCLUSION HCC patients showed a reduced tissue diffusivity when compared with liver haemangioma patients on the ADC map. Tissue diffusivity can be quantitatively assessed by ADC values and helps to differentiate HCC and liver haemangioma. ADC quantification is a valuable tool in oncological practice to characterise and further distinguish different liver lesions, particularly in cases where administration of contrast is contraindicated.

CATEGORY: MCOR 2018: BODY IMAGING

BD002

Tongue cavernous haemangioma

Hairuddin Achmad Sankala¹, Pick Yeen Lai¹

¹Radiology, Hospital Tawau, Malaysia

This case report herein describes our experience of recognising the clinical and imaging features of tongue cavernous haemangioma. A 36-year-old man with no known medical illness presented with macroglossia, which was associated with discomfort. The tongue had progressively increased in size since he was seven years old. However, he was still able to tolerate orally. There were no episodes of bleeding or ulceration. Clinically, there was a diffuse enlargement of the left side of the tongue crossing the midline involving the dorsal, ventral and lateral aspects. The tongue was purplish and had an irregular surface. Multiple hard nodules were palpated. They were non-tender and non-pulsatile. Computed tomography angiography was ordered

and showed a large left-sided tongue mass with multiple hyperdense phleboliths within. The mass had attenuation similar to the adjacent muscles. Linear peripheral enhancement was noted and likely to represent abnormal vascular channels. The mass occupied almost the entire oral cavity, which caused narrowing. Histopathological examination revealed the mass to be a cavernous haemangioma. The patient was planned for surgical reconstruction of the tongue. Recognition of the clinical and imaging features of tongue cavernous haemangioma is crucial so as to make a correct diagnosis and avoid life-threatening biopsies.

CATEGORY: MCOR 2018: BODY IMAGING

BD003

Hughes-Stovin syndrome: a case report

*Isa Azzaki Zainal¹, Zaharudin Haron², Zuhani Abdul Hamid²*¹Radiology, University Kebangsaan Malaysia Medical Centre, ²Radiology, National Cancer Institute, Malaysia

Hughes-Stovin syndrome (HSS) is a very rare clinical disorder of unknown aetiology, although infections and angiodysplasia are among its possible causes. Clinically, patients with HSS present with fever, cough, dyspnoea, chest pain and haemoptysis. Radiological findings of HSS include thrombophlebitis and multiple pulmonary and/or bronchial aneurysms. It is treated either medically or surgically. Medical management includes steroids and cytotoxic agents. In cases of large pulmonary aneurysms, surgical approaches such as lobectomy or pneumonectomy will be carried out. Transcatheter arterial embolisation has emerged as a less invasive alternative to surgery in selected patients with HSS. As aneurysmal rupture is the leading cause of death among patients with HSS, early diagnosis and intervention is essential

to improve the prognosis in these patients. We herein report a case of a 24-year-old man who presented with prolonged fever, joint pain, oral ulcers, headache and blurring of vision. He was diagnosed with Behçet's disease and received high-dose steroids. Contrast-enhanced computed tomography (CECT) of the brain showed extensive dural sinus thrombosis involving the superior sagittal sinus, straight sinus, both transverse sinuses and both sigmoid sinuses. Doppler ultrasonography of the lower limb showed thrombosis within the middle and distal right superficial femoral vein. In view of the non-resolving fever, CECT of the thorax performed a week later revealed two fusiform aneurysms within the posterobasal branch of the right pulmonary artery, which were confirmed via computed tomography pulmonary angiography.

CATEGORY: MCOR 2018: BODY IMAGING

BD004

Troubleshooting the implementation of dual-energy computed tomography pulmonary angiography for the diagnosis of pulmonary emboli at a large level 1 trauma centre

*James Ling¹, John Coucher¹*¹Radiology, Princess Alexandra Hospital, Australia

INTRODUCTION The aim of this study was to evaluate the implementation of dual-energy (DE) computed tomography pulmonary angiography (CTPA) at Princess Alexandra Hospital, Australia.

METHODS All CTPAs performed at the hospital between December 2016 and May 2017 were identified. Signal intensity (presented in Hounsfield units [HU]) was measured at the largest axial image of the main pulmonary artery by a circular region with a diameter of 50%. HU < 210 was considered suboptimal. We compared the image quality of DE and single-energy (SE) CTPAs using chi-square test and two-sided *t*-test. A *p*-value < 0.50 was considered statistically significant.

RESULTS A total of 246 CTPAs (DE: *n* = 175, 71%; SE: *n* = 71, 29%) were identified. In December 2016, mean pulmonary artery signal

intensity of DE CTPAs was significantly lower than that of SE CTPAs (323 HU vs. 364 HU; *p* = 0.02) and the suboptimal scan rate was higher in DE CTPAs than in SE CTPAs (11% vs. 7%; *p* = 0.58). Following these poor results, we identified that the radiographers had chosen the SE contrast protocol for DE CTPAs. After education was provided to the radiographers, improvements to the quality of DE CTPAs were seen in May 2017 – mean pulmonary artery signal intensity improved from 323 HU to 344 HU (*p* = 0.70) and the suboptimal scan rate decreased from 14% to 3% (*p* = 0.04). Both SE and DE CTPAs were of equal quality when evaluated in May 2017 (344 HU vs. 364 HU; *p* = 0.26).

CONCLUSION Human factors should always be considered when troubleshooting quality issues, particularly when new technologies are implemented in a hospital.

CATEGORY: MCOR 2018: BODY IMAGING

BD005

The effect of a modified alternate-day calorie restriction programme on nonalcoholic fatty liver disease

Khairiah Mat Yusoff¹, Juhara Haron¹, Lee Yong Yee¹, Muhammad Izzat Johari¹, Chandran Nadarajan¹, Khairun Nisah Ibrahim¹

¹Radiology, Hospital Universiti Sains Malaysia, Malaysia

INTRODUCTION Nonalcoholic fatty liver disease (NAFLD) is a serious global medical issue. Various diet modifications have been implemented to improve liver steatosis. Shear wave elastography (SWE) is an emerging technique that offers a noninvasive method of liver steatosis assessment. In this study, we aimed to compare the liver steatosis grading and liver elasticity among NAFLD patients who underwent an eight-week modified alternate-day calorie restriction (MADCR) programme.

METHODS Using the Aixplorer® ultrasound system, liver ultrasonography was performed in 39 patients (30 interventional and nine control subjects). Liver steatosis grading, fibrosis grading and SWE of all patients were acquired. Liver steatosis grade and liver elasticity level pre- and post-intervention were compared. Correlation of liver steatosis and grading was analysed using Kendall's tau coefficient.

RESULTS Mean liver steatosis grade and mean fibrosis level of the 30 participants in the intervention group were significantly reduced after the implementation of the MADCR programme. Our results showed that ten patients had improved liver steatosis grading – eight improved from grade 2 to grade 1 and two from grade 1 to grade 0. Our study showed a significant mean difference of liver elasticity in the intervention group after the MADCR programme implementation ($p < 0.001$). From the analysis of the readings for all participants ($n = 78$), SWE values showed a significantly weak correlation with steatosis grading (0–3) of the fatty liver ($p = 0.013$).

CONCLUSION MADCR is beneficial in improving liver steatosis. SWE is a useful and reliable method to assess liver elasticity after intervention.

CATEGORY: MCOR 2018: BODY IMAGING

BD006

Undescended testes: not the end of story, but the beginning

Khor Foo Kiang¹, Hanae Noma Haron², Firdaus Hayati³, Constance Liew Sat Lin¹

¹Medicine-Based Discipline, Faculty of Medicine and Health Sciences, Universiti Malaysia Sabah, ²Radiology, Queen Elizabeth Hospital, ³Surgery, Faculty of Medicine and Health Sciences, Universiti Malaysia Sabah, Malaysia

Abdominoscrotal hydrocele (ASH), also known as herniated hydrocele, is characterised by a fluid-filled mass within the inguinoscrotal and abdominal regions. The condition is more commonly seen in paediatric populations and has a 3.1% incidence rate. The risk of carcinoma in undescended testes is 40 times greater than in normal descended testes. The type of carcinoma for undescended testes is more likely to be seminoma. Ultrasonography is the imaging modality of choice for the paediatric population, whereas computed tomography (CT) of the abdomen is the mode of investigation for adults. Early orchidopexy does not eliminate the risk of malignancy, although it enables early diagnosis of malignancy. We herein present a case of a 32-year-old man with undescended left testis since birth, who had no further imaging performed to locate the undescended testis.

The patient presented with a two-year history of left-sided inguinal swelling, which progressively worsened. Abdominal ultrasonography and CT were performed. Ultrasonography showed a large left-sided hydrocele but was unable to locate the left testis. CT revealed a large retroperitoneal mass with foci of calcifications and central necrosis. The mass encased the main branches of the abdominal aorta. ASH was seen immediately inferior to the retroperitoneal mass, which extended to the left inguinal region. Biopsy was not performed, as the patient defaulted clinic reviews subsequently. Radiological investigation to locate undescended testes is crucial for early surgical orchidopexy and detection of malignant changes. This report thus highlighted the complications and importance of radiological investigation for undescended testes.

CATEGORY: MCOR 2018: BODY IMAGING

BD007

Focal chronic pyelonephritis mimicking renal cell carcinoma: a case report

*Manju T Raja¹, Wan Muhammad Nazief¹, Malinda Abdul Majid¹*¹Radiology, Kuala Lumpur Hospital, Malaysia

Focal pyelonephritis is demonstrated in computed tomography (CT) as an ill-defined focal wedge-shaped area of low attenuation, distinguishable from renal cell carcinoma, which appears as an enhancing renal mass. Variations of radiologic findings are likely due to dynamic changes of the inflammatory process. We herein report a case of a 65-year-old woman with underlying diabetes mellitus who was admitted with a complaint of gross haematuria for one week. Flexible cystoscopy showed cystitis changes. Four-phase renal CT

showed a heterogeneously enhancing left midpole renal mass, which was associated with perinephric fat stranding and thickening of the pararenal fascia. Preoperative diagnosis of renal cell carcinoma was made. Operative findings revealed a renal mass, and histopathologic examination showed chronic glomerulonephritis with heterogeneous areas of infarction and necrosis. In this case, based on the findings of renal mass on CT, focal chronic pyelonephritis was considered as a radiological differential diagnosis.

CATEGORY: MCOR 2018: BODY IMAGING

BD008

A cross-sectional study to assess the agreement between Doppler ultrasonography and nonenhanced magnetic resonance angiography in diagnosing significant main renal artery stenosis and its influencing factors

*Mazeda Murad¹, Nurul Akhmar Omar¹, Bee Yen Ooi¹, Roslina Abd Halim¹*¹Radiology, Seberang Jaya Hospital, Malaysia

INTRODUCTION Doppler ultrasonography (DUS) is the screening tool of choice to detect renal artery stenosis (RAS). In indeterminate cases or when discrepancy exists, magnetic resonance angiography (MRA) is performed. DUS is operator- and skill-dependent. Thus, we conducted this study to: (a) evaluate the agreement between DUS and nonenhanced MRA (NEMRA) in diagnosing significant renal artery stenosis; and (b) determine the factors (e.g. body mass index [BMI], waist circumference and creatinine levels) affecting the agreement.

METHODS We investigated 89 patients (55 males, 34 females; age range 20–89 years) with suspected RAS. DUS was performed using a 3.5-MHz transducer. NEMRA was performed using a 1.5-T machine and reviewed by a radiologist blinded to the DUS results. Peak systolic velocity > 200 cm/s within the main renal artery, acceleration time

> 0.07 seconds and acceleration index < 300 cm/s within the segmental renal arteries are considered as RAS by DUS. Main renal arteries were categorised as normal or significantly stenosed (> 70%) on MRA.

RESULTS A total of 69 patients and 138 main renal arteries were evaluated. There was a 98.8% agreement between DUS and NEMRA for the right renal artery and a 96.5% agreement for the left renal artery. Among the patients, 70.1% were overweight or obese, 36.8% had abnormal waist circumference and 36.8% had abnormal serum creatinine levels. However, BMI, waist circumference and creatinine level were found to have no effect on the agreement.

CONCLUSION There is high agreement between DUS and NEMRA, and thus our results support DUS as a reliable screening examination for RAS.

CATEGORY: MCOR 2018: BODY IMAGING

BD009

Vanek's tumour causing ileoileal intussusception in an adult lady: a case report

Norain Talib¹, Wan Aireene Wan Ahmed¹, Mohd Shafie Abdullah¹

¹Radiology, Universiti Sains Malaysia, Malaysia

Adult presentation of small bowel obstruction caused by intussusception is relatively rare. It is a diagnosis to consider in particular when a patient presents to the emergency department for recurrent abdominal pain. Herein, we report a 49-year-old woman who presented with progressive abdominal pain and showed dilated small bowel on abdominal radiography. Abdominal computed tomography revealed

a bowel-within-bowel appearance of ileoileal intussusception and proximal small bowel faeces sign. Intraoperatively, telescoping of ileal-to-ileal bowel segment was confirmed, with a nodular mass at the antimesenteric border as the leading point. Resection and anastomosis were performed. Histopathological study showed that the leading point mass is a rare inflammatory fibroid polyp known as Vanek's tumour.

CATEGORY: MCOR 2018: BODY IMAGING

BD010

The association of findings from thoracic computed tomography with galactomannan and *Aspergillus*-specific polymerase chain reaction for the diagnosis of invasive aspergillosis in patients with febrile neutropenia

Nurul Ain Mat Idris¹, Juhara Haron¹

¹Radiology, Universiti Sains Malaysia, Malaysia

INTRODUCTION Invasive pulmonary aspergillosis (IPA) shows airway or angio-invasive features on computed tomography (CT). However, those features are nonspecific and diagnosis for IPA should be made in conjunction with the EORTC/MSG criteria. In this study, we evaluated the association of CT findings with galactomannan and *Aspergillus*-specific polymerase chain reaction (PCR) in patients with febrile neutropenia.

METHODS Patients with haematological malignancy who had persistent febrile neutropenia lasting at least three days despite antibiotics underwent thoracic CT within two weeks of clinical diagnosis of IPA. Serum galactomannan assay and *Aspergillus*-specific PCR were performed. Changes in thoracic CT were documented and any associations between mycological findings were analysed

using Fisher's exact test. A p-value < 0.05 was considered statistically significant.

RESULTS A total of 26 patients were enrolled in our study. CT findings for IPA were positive in 17 (65.4%) patients, while 8 (30.8%) of the patients tested positive with serum galactomannan assay and 9 (34.6%) with *Aspergillus*-specific PCR. There was a significant association between PCR and CT findings ($p = 0.009$) but not between galactomannan assay and CT findings ($p = 0.667$).

CONCLUSION A combination of PCR and CT of the thorax may be a reliable noninvasive tool for the early diagnosis of IPA. *Aspergillus*-specific PCR should be considered for inclusion in the EORTC/MSG mycological criteria for the diagnosis of IPA.

CATEGORY: MCOR 2018: BODY IMAGING

BD011

Pancreatic head mass: now you see it, now you don't

*Phyllis Wan Chun Ho¹, Poh Sen Tay²*¹Radiology, Hospital Bintulu, ²Radiology, Sarawak General Hospital, Malaysia

Despite the high prevalence of tuberculosis (TB) worldwide, pancreatic TB is rare. It may present as a solid mass on imaging, mimicking malignancy. Consequently, it represents a diagnostic challenge. This case report suggests that clinicians should have a heightened suspicion when faced with a discrete pancreatic lesion, especially in patients from areas where TB is endemic. A 43-year-old woman presented with a one-month history of epigastric discomfort and anorexia. Abdominal ultrasonography revealed a lobulated, hypoechoic pancreatic mass with multiple liver lesions. Subsequent computed tomography (CT) of the abdomen with pancreatic protocol showed a solid, hypovascular pancreatic head mass with multiple liver lesions. There is, however, no biliary or pancreatic duct obstruction despite the size. A working diagnosis of pancreatic carcinoma or cholangiocarcinoma with liver

metastases was made. The patient was subsequently lost to follow-up, only to present again one year later with fever and cough, in addition to the existing abdominal discomfort. Chest radiography performed during this presentation revealed extensive airspace opacities in both upper lobes and widely scattered miliary nodules. Work-up for TB was carried out, during which the sputum was tested and found to be strongly positive for acid-fast bacilli. Five months following the anti-TB treatment, repeat abdominal CT showed a resolved pancreatic head mass, with partial resolution of the liver lesions and new finding of gross ascites. Unfortunately, the patient succumbed to respiratory failure. The possibility of TB should be considered in the differentials of pancreatic mass and an endoscopic, ultrasonography-guided biopsy may help in the diagnosis of this potentially curable disease.

CATEGORY: MCOR 2018: BODY IMAGING

BD012

Erosive juvenile polyarticular tophaceous gout with hyoid bone involvement

*Shing Ning Chou¹, Phyllis Wan Chun Ho¹, Teik Beng Chuah¹*¹Radiology, Hospital Bintulu, Malaysia

Making a correct and early diagnosis of juvenile gouty arthritis is challenging. To the unwary, the symptom of recurrent, persistent joint pain may be attributed to commoner aetiologies. We herein present a case of an adolescent male with a delayed diagnosis of gouty arthritis and tophaceous involvement of the hyoid bone, which is extremely rare. A moderately built 13-year-old boy presented with a long-standing history of asymmetric polyarthropathy involving the small and large joints of the upper and lower extremities. He received treatment for rheumatoid factor-negative polyarticular juvenile idiopathic arthritis. Despite adequate treatment, he developed multiple painless subcutaneous nodules over the extensor joint surfaces, which were interpreted as rheumatoid nodules. Subsequently, he defaulted follow-up until two years later when he presented with left second-toe ulceration accompanied by a semisolid whitish discharge. Uric acid test was performed and revealed a significantly raised level of uric

acid. Concomitantly, he complained of anterior neck swelling, which was hard in consistency, mimicking neoplasia and chronic infection. Laryngoscopy was unremarkable. Plain radiography showed osteolytic involvement of the hyoid bone. Ultrasonography of the neck showed a heavily calcified neck mass, and contrast-enhanced computed tomography of the neck also revealed a large lobulated nonenhancing calcified anterior midline neck mass surrounding the hyoid bone with associated bony erosion. The patient underwent surgical excision of the mass. Histopathological examination of the mass proved to be gouty tophus. Diagnosis of gout should be considered for refractory painful joints in a patient regardless of age and preexisting diagnosis. Presentation of tophi can be unusual and in unexpected locations. Hence, in patients with coexisting joint pains, a differential of gouty tophus should be considered when they present with neck mass.

CATEGORY: MCOR 2018: BODY IMAGING

BD013

Measurement of middle-ear volume in adults using three-dimensional reconstruction multidetector computed tomography

*Siti Khairunnisaak Abdul Rahman¹, Juhara Haron¹, Mohd Ezane Aziz¹, Nik Adilah Nik Othman²*¹Radiology, ²Otorhinolaryngology, Universiti Sains Malaysia, Malaysia

INTRODUCTION The purpose of this study was to determine the middle-ear volumes (MEVs) in adults of different age groups and genders using three-dimensional (3D) reconstruction multidetector computed tomography (MDCT).

METHODS A total of 140 brain computed tomography (CT) images of adults were retrieved from the picture archiving communications system (PACS). Brain CT was performed using the Siemens SOMATOM Definition AS with a slice thickness of 1 mm and high kernel bone algorithm. Images with complete mastoid air cells were included. Only good-quality images were analysed. Images with abnormality of the skull, brain or ear were excluded. An ear review protocol from the 3D application (using the GE Healthcare PACS Universal Viewer version 5.0 SP6) was used to measure the MEV.

RESULTS Mean right MEV was 3.845 (SD 1.833) cm³ and left MEV was 3.855 (SD 1.843) cm³. The difference between the mean values was not statistically significant (95% CI -0.035 to 0.016; $p = 0.460$). There was also no statistical difference in mean MEVs between male and female patients (right MEV: 95% CI -0.658 to 0.571; $p = 0.889$; left MEV: 95% CI -0.644 to 0.592; $p = 0.934$). Weak negative correlation between MEV and age was observed (right MEV: $r = -0.101$; $p = 0.233$; left MEV: $r = -0.102$; $p = 0.232$).

CONCLUSION This study has provided baseline data on mastoid pneumatization for further studies. We have also shown that MEV measurement using 3D reconstruction MDCT is easily available and reproducible.

CATEGORY: MCOR 2018: BODY IMAGING

BD014

A comparison of the HepaFat-Scan® and the FibroScan® with controlled attenuation parameter in the estimation of hepatic steatosis in patients with nonalcoholic fatty liver disease using histology as the reference standard

*Syaman Harry¹, Anushya Vijayananthan¹, Chan Wah Kheong¹, Yang Faridah¹, Kartini Rahmat¹*¹Radiology, University Malaya Medical Centre, Malaysia

INTRODUCTION We aimed to compare the HepaFat-Scan®, a magnetic resonance (MR) imaging-based technology for the measurement of liver fat, and the FibroScan® with controlled attenuation parameter (CAP) in the estimation of hepatic steatosis in patients with nonalcoholic fatty liver disease (NAFLD).

METHODS Consecutive NAFLD patients who underwent liver biopsy at our institution were enrolled in this study, and had HepaFat-Scan and FibroScan examinations on the same day. Histopathological examinations of liver biopsy specimens were performed by a single expert pathologist who was blinded to the clinical data and reported according to the nonalcoholic steatohepatitis Clinical Research Network scoring system. Area under the receiver operating characteristic curve (AUROC) was used to evaluate the diagnostic accuracy of the HepaFat-Scan and the CAP in the estimation of hepatic steatosis using liver histology as the reference standard.

RESULTS Data of the 72 enrolled patients (mean age 58.3 ± 9.8 years; males 45.8%; mean body mass index 29.9 ± 4.0 kg/m²; central obesity 95.8%) was analysed. The distribution of steatosis was graded as S1, S2 and S3. AUROC (95% CI) for steatosis grades \geq S2 and S3 was 0.90 and 0.85, respectively, for the HepaFat-Scan, and 0.71 and 0.60, respectively, for the CAP. Sensitivity for the diagnosis of steatosis grades \geq S2 and S3 was 84.1 and 27.3, respectively, for the HepaFat-Scan, and 95.6 and 100.0, respectively, for the CAP. Specificity for the diagnosis of steatosis grades \geq S2 and S3 was 81.8 and 72.9, respectively, for the HepaFat-Scan, and 18.2 and 15.1, respectively, for the CAP.

CONCLUSION The HepaFat-Scan has higher accuracy in the estimation of hepatic steatosis in NAFLD patients when compared with the CAP.

CATEGORY: MCOR 2018: BODY IMAGING

BD015

A rare case of biopsied proven renal synovial sarcoma in a young adult patient: a case report and literature review

Wong Sheau Ning¹, Aida Widure Mustapha Binte Mohd Mustapha¹, Zaharudin Haron¹, Malinda Abdul Majid¹

¹Jabatan Pengimejan Diagnostik, Hospital Kuala Lumpur, Pusat Perubatan Universiti Kebangsaan Malaysia, Malaysia

PRIMARY renal synovial sarcoma (PRSS) is very rare and difficult to diagnose. It comprises only 1% of all renal tumours and has a poor prognosis. Despite its rarity, it should be suspected as one of the differentials in the setting of solid-cystic renal masses. Early diagnosis of PRSS is crucial for favourable outcomes. Multiphase renal computed tomography (CT) is an important diagnostic tool prior to surgical interventions. We herein highlight a case of PRSS in a 27-year-old man who presented with painless gross haematuria. Preoperative multiphase renal CT showed a heterogeneous mass at the upper pole of the right kidney. It had a predominantly cystic component with relatively hyperdense areas within it, which

represents a haematoma. We also observed a solid component at the peripheral margin of the mass, which showed significant enhancement in all phases. The preoperative diagnosis was cystic renal cell carcinoma and PRSS was not suspected. Intraoperative findings showed a cystic-tumour in the upper pole of the kidney with areas of haemorrhage and solid growth. Histological and immunohistochemical features were compatible with the diagnosis of synovial sarcoma of the kidney. We discuss the importance of recognising PRSS as one of the crucial diagnoses based on our multiphase renal CT study supported by our review of previous studies.

CATEGORY: MCOR 2018: BREAST RADIOLOGY

BR001

The spectrum of papillary breast lesions in the Malaysian population: radiopathological considerations

Farhana Fadzli¹, Kartini Rahmat¹, Marlina Tanty Ramli², Faizatul Izza Rozalli¹, Mee Hoong See³, Kein Hooi Teoh⁴

¹Biomedical Imaging, University of Malaya Research Imaging Centre, ²Medical Imaging Unit, Faculty of Medicine, Universiti Teknologi MARA,

³Surgery, ⁴Pathology, University Malaya Medical Centre, Malaysia

INTRODUCTION This study aimed to investigate the subtypes of papillary breast lesions in the population of patients at University Malaya Medical Centre (UMMC), Malaysia, via imaging correlations.

METHODS This was a retrospective study to determine the radiopathological features of papillary lesions. A total of 100 patients who had either core biopsy or surgical excision from 2008 to 2012 were identified from the pathology records of UMMC. Among these patients, 28 did not have their imaging records stored in the picture archiving communications system. The available imaging (ultrasonography, mammography and magnetic resonance imaging) for the remaining patients were assessed by a radiologist with five years of experience.

RESULTS The age range of the patients was 21–87 years. 55 patients were diagnosed with intraductal papilloma on histopathological examination, 12 had papillomatosis, five were diagnosed with atypical papilloma, five had papilloma with ductal carcinoma *in situ*, 16 had intraductal papillary carcinoma and seven were diagnosed with invasive micropapillary carcinoma. The correlation between histology and duct changes on ultrasonography was also analysed.

CONCLUSION Patients with breast papillary lesions may represent a significant proportion of patients presenting to surgical clinics, and radiological features may help to predict histology and assist in further disease management.

CATEGORY: MCOR 2018: BREAST RADIOLOGY

BR002

Diagnostic accuracy and clinical feasibility of vacuum-assisted breast biopsy of non-palpable breast lesions: a single-centre experience

Marlina Tanty Ramli¹, Kartini Rahmat², Shaleen Kaur Kirat Singh², Carissa Chan Wai Yee², Anushya Vijayanathan²

¹Medical Imaging Unit, Faculty of Medicine, Universiti Teknologi MARA, ²Biomedical Imaging, University of Malaya Research Imaging Centre, Malaysia

INTRODUCTION In this study, we present our initial experience of utilising vacuum-assisted breast biopsy (VAB) in the diagnosis and treatment of breast pathology.

METHODS All VABs carried out in University Malaya Medical Centre, Malaysia, from March to November 2017 were retrospectively reviewed. The types of procedures and histopathology results were documented. All VABs were performed using the Mammotome device and the Bard® Biopsy Instrument with a ten-gauge biopsy needle.

RESULTS There were 33 stereotactic, 16 ultrasonography (US)-guided and two magnetic resonance (MR) imaging-guided VABs performed. Of the 33 stereotactic VABs, 29 were for suspicious microcalcifications, three for spiculated densities and one for lobulated lesion not seen on US. The number of specimens obtained from stereotactic VABs ranged from 5 to 12. There were 30 benign, two borderline (sclerosing adenosis) and three malignant lesions (two intermediate and one

low-grade ductal carcinoma *in situ*). Out of the 16 US-guided VABs, 15 were performed as therapeutic excisions on 25 lesions that were diagnosed as benign on core needle biopsy. One patient with invasive lobular cancer who was deemed high risk for surgery had US-guided VAB. All lesions measured less than 2.5 cm. The number of specimens obtained from US-guided VABs ranged from 1 to 24. Of the 30 benign lesions, the majority (n = 8) were fibroadenomas. MR imaging-guided VABs were performed on BIRADS category 4 lesions not seen on either mammography or US. 12 specimens were obtained for each of the two MR imaging-guided VABs. Lesions in both VABs were benign.

CONCLUSION The results from our study confirm the high efficiency of VAB in the diagnosis of breast lesions. Diagnosis and treatment using VAB eliminate the need for open surgical procedures, which could decrease the cost of breast disease management and lower morbidity rates.

CATEGORY: MCOR 2018: BREAST RADIOLOGY

BR003

The usefulness and diagnostic accuracy of tomosynthesis in characterising mammographic abnormality

Vithya Visalatchi Sanmugasiva¹, Marlina Tanty Ramli^{1,2}, Kartini Rahmat¹, Farhana Fadzli¹, Caroline Judy Westerhout¹, Yeong Chai Hong¹, Faizatul Izza Rozalli¹, Ng Kwan Hoong¹, Nazimah Abdul Mumin^{1,2}

¹Biomedical Imaging, University of Malaya Research Imaging Centre, ²Medical Imaging Unit, Faculty of Medicine, Universiti Teknologi MARA, Malaysia

INTRODUCTION This study aimed to assess the combined performance of digital breast tomosynthesis (DBT) and two-dimensional full field digital mammography (2DFFDM) in the characterisation of suspicious mammographic abnormalities.

METHODS A retrospective study from September 2014 to May 2017 involving 390 patients with BIRADS categories 4 and 5 lesions who underwent DBT+2DFFDM and biopsy was conducted. Patients with BIRADS category 3 lesions that were biopsied were also included. Characterisation of lesions was based on mass, asymmetry, calcification and associated features, which included architectural distortion, skin thickening, nipple retraction and lymphadenopathy. Histopathology was the gold standard. Sensitivity, specificity, negative predictive value (NPV) and positive predictive value (PPV) were calculated.

RESULTS Of the 390 patients, 243 (62.3%) were in the diagnostic group, 110 (28.2%) in the opportunistic screening group and 37 (9.5%) in the targeted screening group. There were 182 cancers

detected – 154 in the diagnostic group, 19 in the opportunistic screening group and 9 in the targeted screening group. Of the 182 cancers, 76.0% presented as mass, 4.0% as microcalcification only and 20.0% as asymmetric density. Sensitivity, specificity, PPV and NPV for cancer in the detected mass were 93.8%, 85.1%, 88.8% and 91.5%, respectively. PPVs were 61.6% for cancer presenting as microcalcification and 60.7% for focal asymmetric density. PPVs for cancer in BIRADS categories 4 and 5 lesions were 32.2% and 93.1%, respectively. PPVs for cancer in BIRADS subcategories 4a, 4b and 4c lesions were 6.0%, 38.3% and 68.9%, respectively. All biopsied BIRADS category 3 lesions were non-carcinoma.

CONCLUSION DBT+2DFFDM is an effective tool for cancer diagnosis in BIRADS categories 4 and 5 lesions, especially those presenting as masses, with PPVs that are in accordance with the American College of Radiology BIRADS 2013 guidelines. Characteristics of benign-appearing lesions on DBT+2DFFDM show a strong indication of non-malignancy.

CATEGORY: MCOR 2018: BREAST RADIOLOGY

BR004

The impact of multimodality imaging on clinical decision-making in breast cancer patients selected for intraoperative radiotherapy

Wai Yee Chan¹, Kartini Rahmat¹, Shaleen Kaur Kirat Singh¹, Wai Keong Cheah¹, Marlina Tanty Ramli², Farhana Fadzl¹, Mee Hoong See³, Joanne Aisha Mosiun³

¹Biomedical Imaging, University of Malaya Research Imaging Centre, ²Medical Imaging Unit, Faculty of Medicine, Universiti Teknologi MARA,

³Surgery, University of Malaya, Malaysia

INTRODUCTION This study aimed to: (a) correlate the accuracy of lesion size on tomosynthesis, ultrasonography and magnetic resonance (MR) imaging with its operative findings; and (b) compare the detection of multifocal, multicentric and contralateral breast synchronous cancer in standard conventional imaging with that in MR imaging, and its impact on patients' eligibility for intraoperative radiotherapy (IORT).

METHODS 23 patients underwent IORT over an 18-month period. All patients had presurgical tomosynthesis and ultrasonography. Five of these patients had MR imaging in addition to the procedures. The operative outcomes and histopathological findings were documented and compared with imaging findings.

RESULTS Out of the 18 patients who underwent conventional imaging only, 5 (28%) were subjected to external beam radiation therapy (EBRT) after surgery – three had lymphovascular invasion and two had involved margins (the sizes were underestimated on imaging by 7 mm

and 14 mm, respectively). Mean difference between the ultrasonography-measured lesion size and actual pathological size was 2.4 mm, with ultrasonography underestimating the true lesion size. Out of the five patients who underwent preoperative MR imaging, 1 (20%) was subjected to EBRT due to involved margins; the discrepancy between lesion size in pathology and in MR imaging was 13 mm. IORT was not suitable for two patients due to the detection of multicentric disease in the breast and axillary tail; one patient underwent mastectomy while the other did not undergo surgery. Mean difference between MR imaging size and pathological size was 0.5 mm. No additional satellite nodules were found intraoperatively in all patients.

CONCLUSION Standard conventional imaging shows good lesion size correlation with operative findings. Preoperative MR imaging is also a useful adjunct and has an impact on decision-making regarding patients' eligibility for IORT.

CATEGORY: MCOR 2018: MUSCULOSKELETAL

MS001

The unique 'dot-in-circle' sign on magnetic resonance imaging in a case of Madura foot

Apsara Panicker¹, John George²

¹Radiology, Kuala Lumpur Hospital, ²Biomedical Imaging, University Malaya Medical Centre, Malaysia

Mycetoma or Madura foot is a chronic subcutaneous granulomatous infection caused by fungi or aerobic bacteria. The disease commonly affects the feet and spreads to involve the deeper structures and bones, resulting in destruction, deformity and loss of function. We herein report a case of a histologically proven Madura foot in a Malaysian Indian woman with severe infection who required amputation, and the associated specific 'dot-in-circle' sign seen on preoperative magnetic resonance (MR) imaging. A 61-year-old woman presented with complaints of a progressive painful swelling of the right foot with recurrent discharge. Symptoms began eight years prior, initially presenting as a painless nodular growth on the sole of her foot, which worsened. She had no significant history of trauma to her foot prior to her initial symptoms. She received numerous in- and outpatient

treatments for recurrent discharges, soft tissue infection and osteomyelitis. Initial tissue and culture samples were negative. However, four years ago, pus culture and histopathology report of a skin biopsy confirmed the diagnosis of Madura foot. Laboratory tests were unremarkable except for a raised erythrocyte sedimentation rate. We further described the plain radiograph and MR imaging findings of this patient's foot, the latter of which demonstrated the characteristic 'dot-in-circle' sign. This case represents a severe case of actinomycetoma that required amputation. Early diagnosis is therefore essential. MR imaging with the unique, pathognomonic and easily recognisable 'dot-in-circle' sign allows for early diagnosis and should therefore be performed in cases of chronic nonhealing foot infections or suspected cases of mycetoma without positive biopsy or microbiology.

CATEGORY: MCOR 2018: MUSCULOSKELETAL

MS002

Multiple enchondromatosis (Ollier disease): a rare case in the Philippines

*Ernie Bautista II¹*¹Radiology, Quezon City General Hospital, the Philippines

We herein present a case of Ollier disease (multiple enchondromatosis), which is an extremely rare nonhereditary sporadic disorder in which intraosseous benign cartilaginous tumours (enchondroma) develop close to the growth plate cartilage. The global prevalence rate of the condition is estimated at around 1 in 100,000. Due to a paucity of peer-reviewed research and the rarity of Ollier disease in the Philippines, its incidence rate was rarely documented. A 23-year-old man presented to the Quezon City General Hospital emergency department due to a vehicular (motorcycle) accident. The patient sustained some limitations in the range of motion in his right shoulder. Radiographic examinations revealed no evidence of

radiologic fracture, but there was an incidental finding of multiple well-defined, osteolytic, expansile lesions with bony outgrowth in both the upper and lower extremities. A radiologic diagnosis of multiple enchondromatosis was made based on the morphology and location of the bone lesions seen on plain radiography. The patient was managed conservatively and advised with serial radiologic follow-ups. This case report shows the importance of early diagnosis, timely intervention and treatment of Ollier disease, and represents one of the very rare cases of multiple enchondromatosis reported in the Philippine literature.

CATEGORY: MCOR 2018: MUSCULOSKELETAL

MS003

An uncommon presentation of a giant cell tumour

*Hon Keong Chang¹, Alex Fook Seng Lee², Norzailin Abu Bakar¹*¹Radiology, Hospital Universiti Kebangsaan Malaysia, ²Radiology, Kuala Lumpur Hospital, Malaysia

Giant cell tumour (GCT) is a benign but locally aggressive tumour. This often causes challenges in ascertaining the diagnosis, especially in the case of atypical presentations. GCTs of the talus or multicentric GCTs are rare. We herein report a case of a 19-year-old woman with a GCT of the left talus associated with multicentricity. No abnormality was detected during blood investigations. The diagnosis was made in

correlation with the radiological and histopathological findings. She underwent curettage and bone grafting for the left talar lesion and recovered well. However, she developed multiple lesions later and was required to undergo wide excision and prosthesis insertion. In this report, we stressed the importance of imaging modalities and correlations with histopathological findings in the diagnosis of GCTs.

CATEGORY: MCOR 2018: MUSCULOSKELETAL

MS004

A correlation between ultrasonographic dynamic evaluation and clinical laxity grading of anterior talofibular ligament and calcaneofibular ligament tears among athletes

*Indar Rahini Hairi¹, John George¹, Zulkarnain Jaafar²*¹Biomedical Imaging, ²Sports Medicine, University Malaya Medical Centre, Malaysia

INTRODUCTION This study aimed to find a correlation between clinical grading and ultrasonographic dynamic grading of anterior talofibular ligament (ATFL) and calcaneofibular ligament (CFL) tears.

METHODS A total of 35 patients were recruited for sports-induced lateral ankle sprain injuries. The patients were first assessed clinically by a sports medicine specialist. The anterior drawer test was used to assess the integrity of the ATFL and the talar tilt test was used to assess the CFL clinically. Clinical grading was divided into three: Grade I – no ligament laxity (normal); Grade II – some degree of laxity but with a firm endpoint (partial tear); and Grade III – gross laxity without an endpoint (complete tear). Subsequently, an ultrasonographic assessment was done by a radiologist who was blinded to the clinical grading results. Ultrasonographic grading ranged from a scale of I to III: Grade I indicated normal; Grade II was for partial thickness

tear; and Grade III was for a complete tear. Statistical analysis was performed using Spearman's rank correlation coefficient to correlate both findings.

RESULTS There was a strong correlation between the anterior drawer test and the dynamic ATFL ultrasonographic grading ($n = 0.58$), and between the talar tilt test and dynamic CFL ultrasonographic grading ($n = 0.69$).

CONCLUSION We found a strong positive correlation between the clinical and ultrasonographic gradings in evaluating ATFL and CFL tears. The anterior drawer test and talar tilt test are useful clinical screening tests for evaluating lateral sprain injuries. Dynamic ultrasonography is an important diagnostic tool to assess ligament tears, as it has been proven to show a high resolution of the anatomy and pathology of lateral ankle ligaments.

CATEGORY: MCOR 2018: MUSCULOSKELETAL

MS005

A case of osteogenesis imperfecta

*Jerik Yumol¹*¹Radiology, Quezon City General Hospital, the Philippines

Osteogenesis imperfecta (OI) is a rare inherited connective tissue disorder with a broad spectrum of medical and genetic variability. The inherent diversity in the majority of cases involves mutations in the type I collagen protein (*COL1A1* and *COL1A2* genes). The progressive deforming type is OI type III. We herein present a case of a 43-year-old woman who presented with diarrhoea, and with an incidental note of severe dwarfism and body disproportion associated with mobility impairment. Radiological examinations revealed generalised osteopenia, marked kyphoscoliosis of the spine, protrusio acetabuli, multiple pathologic fractures and long bone deformities, all of which are suggestive of OI type III. The atypical presentation of this condition in adulthood necessitated an early diagnosis for prompt intervention.

However, treatment for OI is not curative but focuses on improving the quality of a patient's life. The clinical sequela of this anomaly is brittle bones, which predispose the patient to recurrent fractures even in trivial trauma. Clinical and radiographic findings of short stature, white sclerae, hearing loss, severe kyphoscoliosis and Roentgen images that reveal generalised osteopenia, multiple pathologic fractures, long bone deformities and thin ribs are vital findings in diagnosing this rare condition. OI is among the few medical conditions that can be satisfactorily diagnosed based on history-taking and radiographic imaging. A multidisciplinary approach to treatment is valuable in improving the patient's quality of life since there is currently no known cure for OI.

CATEGORY: MCOR 2018: MUSCULOSKELETAL

MS006

Multidetector computed tomography arthrography of the shoulder is a better cost-saving imaging modality in suburban hospitals: a pictorial essay

Ming Huan Cheng^{1,2}, Eun Kyung Khil², Jung-Ah Choi²

¹Radiology, Hospital Keningau, Malaysia, ²Radiology, Hallym University Medical Centre, Sacred Heart Hospital, South Korea

Computed tomography (CT) arthrography of the shoulder has been underutilised in both suburban and major hospitals due to the greater preference for shoulder magnetic resonance (MR) imaging among clinicians. In many hospitals, this results in long patient waiting lists, and some patients from rural areas are not able to undergo MR imaging due to accessibility problems. Studies have shown that multidetector CT (MDCT) arthrography of the shoulder is as sensitive as MR imaging in diagnosing shoulder rotator cuff injury. In this pictorial essay, we present MDCT shoulder arthrography imaging findings and compare them with findings from MR imaging of the shoulder. We selected 20 cases in which MDCT arthrography, including various arthrography

techniques, and MR imaging of the shoulder were performed. The images demonstrated rotator cuff injury, glenoid labrum pathology and associated degenerative features. All imaging modalities were performed in the Radiology Department, Hallym University Medical Center, Sacred Heart Hospital, South Korea, between January 2014 and December 2016. MDCT arthrography of the shoulder was proven to be good in diagnosing rotator cuff injuries, superior labral anteroposterior lesions and instability. It is a preferred modality in suburban hospitals without MR imaging facilities, as it is cost-saving and provides faster examination time. In addition, more patients from rural areas are able to undergo MDCT arthrography in nearby hospitals.

CATEGORY: MCOR 2018: MUSCULOSKELETAL

MS007

Thrower's fracture: a rare injury from a rare sport in Malaysia

Mohd Shukry Mohd Khalid¹, Sabrilhakim Sidek¹

¹Medical Imaging Unit, Faculty of Medicine, Universiti Teknologi MARA, Malaysia

Herein, we report a rare sports injury occurring in an amateur dodgeball player and aim to raise awareness of this injury in order to avoid unnecessary investigations. Dodgeball is a relatively new sport in Malaysia. The game started gaining popularity recently, with both the national men's and women's teams winning medals in the World Dodgeball

Championship in Australia in 2016. A 23-year-old amateur dodgeball player, who sustained a spontaneous fracture of the right humerus after throwing the ball during his training session, presented at our institution. We discuss the mechanism of injury, radiological investigation and management of this rare sports injury.

CATEGORY: MCOR 2018: MUSCULOSKELETAL

MS008

Cadaveric stature estimation in the Malaysian population using postmortem computed tomography

Sabrilhakim Sidek¹, Mansharan Kaur Chainchel Singh^{1,2,3}, Afrina Aqilah Abd Shukor¹, Nur Najla Aqilah Jamil¹, Mas Aina Mohd Nasir¹, Muhammad Azrul Talib¹, Lai Poh Soon³, Saiful Nizam Abdul Rashid^{3,4}, Mohamad Helmee Mohamad Noor³, Siew Sheue Feng³

¹Faculty of Medicine, ²Institute of Pathology, Laboratory and Forensic Medicine, Universiti Teknologi MARA, ³National Institute of Forensic Medicine, Kuala Lumpur Hospital, ⁴Parkcity Medical Centre, Ramsay Sime Darby Healthcare, Malaysia

INTRODUCTION Postmortem computed tomography (PMCT) plays an established role in forensic investigation of dead bodies. Previous published studies estimated the stature of African-Americans and Caucasian Americans, and Japanese populations using skeletal spine length from postmortem cases. However, there was no published study to estimate the stature for other populations or races. Therefore, this study was performed to assess the correlation between skeletal spine lengths and actual heights, and to derive novel regression formulas for stature estimation among dominant races in Malaysia.

METHODS A total of 115 postmortem cases were obtained retrospectively from 2015. These cases were scanned using multislice computed tomography. Actual heights were obtained from our PMCT database. Curved multiplanar reformatted imaging and three-dimensional image

reconstructions were performed, followed by measurement of the whole spine length (WSL), and the length of cervical (CL), thoracic (TL) and lumbar (LL) spine segments using the OsiriX software. All statistical analyses were performed using SPSS version 22.0.

RESULTS Statistical analyses showed positive correlations between WSL, CL, TL, LL and the actual height. WSL showed the highest correlation with actual height, followed by CL, TL and LL. With regard to the specific spine segment groups, CL yielded a better correlation with actual height compared to TL and LL. Separate regression formulas for stature estimation were obtained for the dominant races in Malaysia.

CONCLUSION Our results showed that skeletal spine length can be used as an alternative tool for stature estimation. The remaining CL may be used for stature estimation when the WSL is not retrievable.

CATEGORY: MCOR 2018: MUSCULOSKELETAL

MS009

Morphologic changes of the rotator cuff muscles following fast isokinetic training in state-level weightlifters

Siti Salwa Mohamad Zaini¹, Khairil Amir Sayuti¹, Mohd Ezane Aziz¹

¹Radiology, Universiti Sains Malaysia, Malaysia

INTRODUCTION This study aimed to evaluate the size of the rotator cuff muscles and muscle-fibre angle of the supraspinatus muscle (SS) in two different types of exercise – fast isokinetic training (FIT) and traditional isotonic training (TOT) – in state-level weightlifters.

METHODS Athletes (n = 16) were recruited through Majlis Sukan Negeri Kelantan, a sports council in the state of Kelantan, Malaysia. They were gender- and weight-matched and randomly assigned to either the TOT or FIT group. Both groups went through a total of 24 training sessions – three sessions per week for eight weeks. Magnetic resonance (MR) imaging of the rotator cuff muscles was performed on the athletes before the commencement of the training programme and after the programme ended. Measurements of muscle cross-sectional area (CSA) and muscle-fibre pennation angle (PA) were also taken.

RESULTS CSAs of the four rotator cuff muscles increased after the intervention programme, and significant improvements ($p < 0.05$) were found in the CSAs of the SS and infraspinatus and teres minor muscle (ISTM), but not in the subscapularis muscle (SC). Significant increments in CSAs were also found in the rotator cuff muscles of all athletes who underwent FIT. However, for those who underwent TOT, significant increments in CSAs were found only in the SS, but not in the SC and ISTM. PAs of the SS significantly increased after the intervention programme. Significant increments in PAs were found in the rotator cuff muscles of all athletes, regardless of their training programme.

CONCLUSION FIT results in significant increments in CSAs of the four rotator cuff muscles. Significant increments in PAs were found in the rotator cuff muscles of all athletes who underwent either FIT or TOT.

CATEGORY: MCOR 2018: NEURORADIOLOGY

NR001

Neuroimaging abnormalities in anti-NMDA receptor encephalitis

Alan Basil Peter^{1,2}, Norlisah Ramli², Kartini Rahmat², Li Kuo Tan², Chong Tin Tan³, Suhailah Abdullah³, Kheng Seng Lim³

¹Medical Imaging, Faculty of Medicine, Universiti Teknologi MARA, ²Biomedical Imaging, University of Malaya Research Imaging Centre, ³Neurology, Faculty of Medicine, University of Malaya, Malaysia

INTRODUCTION This study aimed to: (a) identify pathognomonic changes using neuroimaging in patients with anti-NMDA receptor encephalitis; (b) look for subtle changes in serial imaging of these patients; (c) determine if there is any loss of brain volume during the course of the illness; and (d) evaluate the usefulness of diffusion tensor imaging (DTI) in detecting damage to the tracts within the brain.

METHODS Four patients with anti-NMDA receptor encephalitis and four age-matched normal subjects underwent clinical functional assessment and two serial magnetic resonance imaging in a 3.0T scanner – once at the time of presentation and once three months later. Whole brain volumes were calculated using voxel-based morphometry analysis. The DTI dataset was post-processed by the MRICConvert, FSL and AFNI software to obtain mean fractional anisotropy (FA), mean diffusivity (MD), axial diffusivity (AD) and radial diffusivity (RD).

RESULTS One anti-NMDA receptor encephalitis patient showed mild functional impairment, while the rest showed no functional impairment at nine months follow-up. Our study did not show any specific pattern of brain volume change in the patients. We observed trends of lower mean FA values and higher mean MD, AD and RD values in the majority of the 50 tracts studied in the anti-NMDA receptor encephalitis patient group. However, only a few were statistically significant.

CONCLUSION Our four patients recovered well. Whole brain volumes did not demonstrate significant temporal changes that differed from the control group. DTI assessment showed trends that suggest damages to the neuronal integrity in the patient group. Serum antibody tests remain essential in diagnosing anti-NMDA receptor encephalitis. However, DTI may shed light on grading the severity of disease and assessing patients' response to treatment.

CATEGORY: MCOR 2018: NEURORADIOLOGY

NR002

Computed tomography and magnetic resonance imaging of the brain in MELAS syndrome: a case report

Andrew Cheng¹, Yan Lin Li¹, Mabel Tong²

¹Radiology, Queen Mary Hospital, ²Radiology, North District Hospital, Hong Kong

MELAS (mitochondrial encephalopathy, lactic acidosis and stroke-like episodes) syndrome is a rare multisystem disorder caused by mitochondrial DNA mutations. MELAS syndrome typically occurs at between 4 and 15 years of age. Early symptoms of the disease are varied and nonspecific, which complicate the diagnosis. We herein present a case of a woman with MELAS syndrome and discuss the typical radiological findings of this rare condition. A 35-year-old woman reported having recurrent headache and memory deficit, psychomotor retardation and cognitive impairment since the age of 15 years. She presented with repeated seizures, right hemiplegia and dysphasia. Computed tomography showed symmetrical bilateral globus pallidus calcifications. Magnetic resonance (MR) imaging showed generalised cerebral atrophy. Cerebral infarcts with non-vascular territories were noted in bilateral temporoparietal-occipital lobes. Biochemical

marker showed metabolic acidosis and lactic acidosis. Skeletal muscle biopsy findings were consistent with mitochondrial myopathy. Strongly succinate dehydrogenase-reactive blood vessels were noted, which suggested MELAS syndrome. Genetic clinical report showed A3243G mutation. The patient was diagnosed with MELAS syndrome based on the clinical, radiological and pathological findings. She was put on coenzyme Q10, creatine and L-arginine. She was also dependent on her father for her activities of daily living. MELAS syndrome is a rare disease with an early onset (before the age of 40 years). Brain imaging typically shows cerebral atrophy, cerebral infarcts within non-vascular territories and symmetrical basal ganglia calcifications. Final diagnosis can be assisted by skeletal muscle biopsy, MR spectroscopy for lactate peak at 1.3 ppm and positive point mutation for A3243G in genetic screening.

CATEGORY: MCOR 2018: NEURORADIOLOGY

NR004

Regional diffusion tensor imaging-derived tensor metrics obtained from white matter tracts for the characterisation of gliomas

Pohchoo Seow¹, Aditya Hernowo², Vairavan Narayanan², Jeannie Hsiu Ding Wong¹, Norlisah Ramli¹

¹Biomedical Imaging, ²Surgery, University of Malaya, Malaysia

INTRODUCTION This study aimed to investigate diffusion tensor imaging (DTI)-derived tensor metrics obtained from white matter (WM) tracts of the surrounding- and within-tumour regions for the grading of gliomas.

METHODS A total of 24 histologically proven glioma patients underwent a standard magnetic resonance (MR) imaging tumour protocol with DTI. The intratumoural, peritumoural and tumour subregion masks were delineated using the snake model (ITK-SNAP) with structural MR images (T1-weighted, T2-weighted and fluid-attenuated inversion recovery sequences) as reference. Data derived from DTI processing and diffusion tensor fitting generated the DTI metric maps. Tractography was performed to delineate the WM tracts in both regions. Mean values of DTI metrics, such as fractional anisotropy, mean diffusivity (MD), axial diffusivity (AD), radial diffusivity

(RD), pure isotropic diffusion (p), pure anisotropic diffusion, total magnitude of diffusion tensor (L), linear tensor, planar tensor, spherical tensor and relative anisotropy, were obtained from mapping the WM tracts on the DTI metric maps.

RESULTS Significant differences were demonstrated in a few DTI metrics in the solid enhancing subregions (MD, AD, RD and p) and solid nonenhancing subregions (MD, AD, RD, p and L) between different tumour grades.

CONCLUSION Our study suggested that the WM tracts were not completely destroyed but were still intact inside the tumour, even for glioblastoma multiforme, as opposed to the common belief that tracts are completely destroyed. DTI metrics provide insights on regional WM tract impairment in the presence of tumour, while preoperative identification of WM tracts can improve neurosurgical planning.

CATEGORY: MCOR 2018: NEURORADIOLOGY

NR005

Malignant melanoma of the nasal cavity

Rofiah Ali¹, Tan Chai Hoong¹

¹Radiology, Sungai Buloh Hospital, Malaysia

Nasal cavity and paranasal sinus cancers are rare and account for approximately 0.2%–0.5% of malignant tumours. Squamous cell carcinoma presents as the commonest histology of sinonasal malignancy. Malignant melanoma comprises less than 1% of sinonasal cavity tumours. Patients usually present with nasal obstruction, epistaxis or nasal discharge, and rarely with pain. Malignant melanoma of the nasal cavity is a challenge to diagnose due to the nonspecific clinical features and obscure location. We herein report a case of intranasal melanotic malignant melanoma for its rarity and unusual age of presentation. A 35-year-old woman with no known medical history presented with a sudden onset of painless epistaxis that lasted for two days. Urgent computed tomography (CT) of the paranasal sinuses showed a large soft-tissue mass with peripheral enhancement filling the right nasal

cavity. Endoscopic examination revealed a dark mass at the posterior one-third aspect of the right inferior turbinate. Repeat CT for preoperative staging revealed a markedly enhancing, superficial small lesion at the right inferior turbinate after careful scrutiny and adjustment of CT windowing. The patient underwent endoscopic medial right maxillectomy. Subsequently, she was referred for oncology treatment. However, she defaulted treatment and presented later on with metastases to the chest wall, breast and retroperitoneum. This case illustrates the challenge in diagnosing a small nasal mucosal melanoma in the presence of surrounding haematoma and obscure location. Endoscopic examination and histological diagnosis are complementary to imaging and essential for diagnosing early-stage tumour.

CATEGORY: MCOR 2018: NEURORADIOLOGY

NR006

Microstructural integrity of the peripheral nerves in Charcot-Marie-Tooth disease: a magnetic resonance imaging evaluation study

Thiagu Krisnan¹, Faizatul Izza Rozalli¹, Farhana Fadzli¹, Norlisah Ramli¹, Kartini Rahmat¹

¹Radiology, University Malaya Medical Centre, Malaysia

INTRODUCTION Charcot-Marie-Tooth (CMT) disease is a common inherited neurological disorder, which results in peripheral neuropathy. Our goal was to investigate the microstructural integrity of sciatic and peroneal nerves in CMT disease using diffusion tensor imaging (DTI) and evaluate muscle atrophy severity in CMT disease using magnetic resonance (MR) imaging.

METHODS A total of 18 patients (nine CMT disease patients and nine age-matched healthy controls) were prospectively recruited. MR imaging-DTI was performed to evaluate the sciatic and peroneal nerves. Images were post-processed to obtain DTI values. Axial in-phase and out-of-phase sequences of the calf were used to classify muscle atrophy on the tibialis anterior muscle.

RESULTS A significant difference was found between the DTI values (fractional anisotropy [FA] and radial diffusivity [RD]) of CMT disease patients and that of controls in both sciatic and peroneal nerves. In CMT patients, the FA value was significantly reduced and the RD

value was significantly increased in both sciatic and peroneal nerves (FA: $p < 0.001$; RD: $p = 0.004$). Mean muscle atrophy of the tibialis anterior muscle was significantly reduced in CMT disease patients as compared to that of controls ($p < 0.001$). We also found statistical significance between neuropathy severity and muscle atrophy grading, with the highest correlation observed between FA values of sciatic and peroneal nerves ($r = -0.7$; $p < 0.001$).

CONCLUSION MR imaging-DTI was able to detect degenerative and demyelination changes in patients with CMT disease, which corresponds to the nature of the illness. In our study, MR imaging also showed that there was significant muscle atrophy in CMT disease patients as compared to controls. In the future, MR imaging-DTI could be a useful screening tool for asymptomatic high-risk patients with family histories of CMT disease, and could help in the early detection of neuropathy and early intervention of progressive neuropathy.

CATEGORY: MCOR 2018: NEURORADIOLOGY

NR007

Vein of Galen aneurysmal malformation: a case of an uncommon intracranial vascular malformation and literature review

Yeong Huei Yiaw¹, Teck Chong Yap¹, Aida Mastura Mustapha¹, Aun Nee Lim¹, Bee Shuang Lee², Ann Cheng Wong²

¹Diagnostic Radiology, ²Paediatrics, Sarawak General Hospital, Malaysia

Vein of Galen aneurysmal malformation (VGAM) is a rare form of vascular malformation in neonates. We herein present a case of a premature newborn with an incidental finding of intracranial vascular malformation. An antenatally uneventful premature neonate with a gestation period of 34 weeks and 3 days presented to the hospital with several neonatal jaundice and required exchange transfusion. Bedside cranial ultrasonography screening detected intracranial vascular malformation, and thus the patient was suspected with VGAM. Cardiac echocardiography showed a structurally normal heart with good cardiac function. However, dilated coronary sinus was present. Diagnosis was then reaffirmed with magnetic resonance

(MR) angiography and MR venography. The patient was treated in the neonatal intensive care unit for congenital pneumonia and severe neonatal jaundice with acute kidney injury. Since the patient had no significant cardiac failure symptoms, cerebral digital subtracted angiography and therapeutic embolisation were withheld. The findings of cranial ultrasonography and MR imaging of the brain are presented in this report, followed by a literature review of this unusual vascular malformation. Knowledge of this rare entity, and the use of ultrasonography and MR imaging are beneficial in the diagnosis of this infrequent intracranial vascular malformation and future planning for further disease management.

CATEGORY: MCOR 2018: NEURORADIOLOGY

NR008

A rare case of tectal plate glioma with a typical presentation of obstructive hydrocephalus

Yuh Yang Leong¹, Hamzaini Abdul Hamid¹, Shahizon Azura Mohamed Mukari¹

¹Radiology, Pusat Perubatan Universiti Kebangsaan Malaysia, Malaysia

Tectal plate lesions are rare, and their aetiology varies from neoplastic, vascular, infectious to inflammatory in nature. Even though lesions in the tectal plate are small in size, they could cause significant mass effect, leading to obstructive hydrocephalus, due to their proximity to the aqueduct of Sylvius. The subtlety of these lesions' radiological appearance might escape the untrained and unsuspecting eye. Histopathological confirmation via surgical biopsy of the brainstem, which is referred to as the 'no man's land', is not without risks. We herein present a case in which a male adolescent presented with headache, fever and behavioural changes, which are symptoms mimicking meningoencephalitis. Subsequent imaging showed a small tectal plate lesion; its radiological features were supportive of a tectal plate low-grade glioma causing acute obstructive hydrocephalus. The patient recovered well after a cerebrospinal fluid

diversion procedure via shunt placement. A conservative approach was taken in this case in view of the benign radiological appearance of the lesion. The patient was discharged well. Follow-up imaging showed radiological stability of the lesion, further supporting the diagnosis of a low-grade tumour. Detailed scrutiny of the images, especially along the pathway of the ventricular cerebrospinal fluid flow, with a high index of suspicion is required, as low-grade tectal gliomas tend to demonstrate subtle radiological findings and could be missed, especially since they are small and do not cause significant distortions to the normal anatomy. Radiological diagnosis plays a significant role in such cases, as the risk of surgical biopsy of the brainstem for histopathological examination may outweigh the benefits.

CATEGORY: MCOR 2018: PAEDIATRIC RADIOLOGY

PD001

Establishing the reference value for normal liver stiffness among healthy children assessed by point shear wave elastography imaging

Kuan Siong Sim¹, Roziah Muridan¹, Anushya Vijayananthan¹

¹Radiology, University Malaya Medical Centre, Malaysia

INTRODUCTION Ultrasound shear wave examination using the ElastPQ® technique (Philips Healthcare, Bothell, WA, USA) is a new noninvasive method of assessing liver fibrosis by measuring liver stiffness. We aimed to determine the reference value of normal liver stiffness among healthy children in Malaysia via point shear wave elastography, and to establish a correlation between normal liver stiffness and age, gender and ethnic group. We also assessed the feasibility and limitation of shear wave elastography in the paediatric population.

METHODS A total of 115 healthy children between the ages of one month and 12 years were examined using the ElastPQ technique for the measurement of liver stiffness. For every child, ten ElastPQ measurements were obtained in both lobes of the liver through the intercostal space. A median of ten ElastPQ measurements was analysed and

correlated to age group, gender and ethnic group. Medians, standard errors of means, and correlations between median liver stiffness and other study variables were calculated. Information regarding the potential limitations of this examination was also collected.

RESULTS There were statistically significant differences in median liver stiffness between the different age groups (1 month–2 years: 0.69 ± 0.12 kPa; 3–5 years: 2.61 ± 0.30 kPa; 6–11 years: 3.44 ± 0.19 kPa; 12 years: 4.33 ± 0.44 kPa); liver stiffness increased with age ($r = 0.644$; $p < 0.01$). Gender and ethnic group had no significant effect on liver stiffness.

CONCLUSION ElastPQ shear wave elastography is an easy noninvasive method for the measurement of liver stiffness in paediatric populations and a promising tool in the diagnosis of liver fibrosis.

CATEGORY: MCOR 2018: PAEDIATRIC RADIOLOGY

PD002

Orbital manifestations of Langerhans cell histiocytosis: a case report

*Nur Asma Sapiai¹, Juhara Haron²*¹Radiology, Hospital Kuala Krai, Ministry of Health, ²Radiology, Universiti Sains Malaysia, Malaysia

Langerhans cell histiocytosis (LCH) is a spectrum of disorders characterised by the accumulation of histiocytes in various tissues. It is rarely encountered in ophthalmic practice. We herein report a case of a six-month-old Malay boy who presented with swelling and redness in the upper orbital ridge of his right eye for one week, which was associated with right eye watery discharge. The patient was also feverish. Clinically, the swelling was firm in consistency, neither mobile nor tender, and the underlying skin was normal. He was treated for right upper lid abscess and prescribed antibiotics. However, the swelling progressively increased in size one week after he had completed his two-week antibiotics course. Skull radiography showed erosion of the superolateral aspect/wall of the right orbital rim. Computed tomography of the brain and orbit showed a lobulated,

homogeneously enhancing, hyperdense soft-tissue mass, which occupied the superolateral aspect/wall of the right orbital rim. The mass was associated with lytic lesion destruction of the right orbital rim and greater wing of the sphenoid bone. There was no calcification or cystic component within the mass. A differential diagnosis of neuroblastoma metastasis or LCH was made on the basis of the mass that occupied the superolateral aspect/wall of the right orbital rim. The patient underwent right superotemporal orbital mass incisional biopsy. Histopathological examination confirmed the diagnosis of LCH. LCH should be considered as a differential diagnosis when imaging techniques in paediatric patients reveal craniofacial and skull base osteolytic lesions with soft-tissue components.

CATEGORY: MCOR 2018: PAEDIATRICS RADIOLOGY

PD003

Biliary rhabdomyosarcoma: a diagnostic challenge

*See Khim Sim¹, Nik Fatimah Salwati Nik Malek¹, Mohan Arunasalam A Nallusamy²*¹Radiology, ²Paediatric Surgery, Hospital Sultanah Bahiyah, Malaysia

Rhabdomyosarcoma is a rare cause of obstructive jaundice in children. However, it is considered to be the most common biliary tract tumour in children. We herein describe the case of a 16-month-old girl who presented with obstructive jaundice and was referred to the paediatric surgical department of our hospital, where biliary tree tumour was ruled out. Intraoperative and histological features confirmed the diagnosis of rhabdomyosarcoma. Postoperatively, the patient was referred to the oncology team for further treatment. Making a diagnosis of biliary rhabdomyosarcoma solely based on radiological features

remains challenging. Diagnostic imaging modalities, including ultrasonography, computed tomography and magnetic resonance cholangiopancreatography, are advantageous and important in helping to establish an accurate diagnosis and evaluate the extent of rhabdomyosarcoma, which involves the biliary tree, when considering different surgical approaches. A multidisciplinary treatment approach of appropriate surgical interventions, chemotherapy and radiotherapy has improved the prognosis and long-term survival of patients with rhabdomyosarcoma.

CATEGORY: MYSIR 2018: INTERVENTIONAL RADIOLOGY (NON-NEUROLOGICAL)

MY001

The correlation between arteriovenous fistula stenosis and haemodialysis parameters before and after angioplasty

*Ani Darwina Abd Halim¹, Azreen Syazril², Juhara Haron¹*¹Radiology, ²Nephrology, Universiti Sains Malaysia, Malaysia

INTRODUCTION Angioplasty helps in maintaining the patency of the arteriovenous fistula (AVF). However, improvements to the percentage of stenosis and haemodialysis functions are still questionable. In this study, we aimed to look for correlations between the percentage of residual stenosis and haemodialysis success.

METHODS A total of 47 patients underwent angioplasty in the Advanced Minimally Invasive Endovascular and Neurointervention Unit, Universiti Sains Malaysia, Malaysia, from June 2014 to October 2015. However, 14 patients were excluded from the final analysis and 19 were lost to follow-up, which left a total of 14 patients enrolled in our study. Images from the picture archiving communications system were reviewed by a radiologist. Three measurements were taken: (a) diameter of the stenotic vessel before angioplasty (measured at the most stenosed segment); (b) diameter of the normal adjacent venous limb; and (c) diameter of the stenotic vessel after angioplasty (measured at the same site as in [a]). At least three different measurements

were taken at different times for each measured diameter and the calculated mean was taken as the final measurement. Following that, the pre- and post-angioplasty percentages of stenosis were calculated. The last haemodialysis through the AVF prior to angioplasty was taken as pre-angioplasty parameters and the first haemodialysis after angioplasty through the intervened AVF was taken as post-angioplasty parameters.

RESULTS All 14 subjects had significant stenosis before angioplasty. Technical success was achieved in 57.1% of patients after angioplasty. There was a weak correlation between the percentage of stenosis and blood pump flow rate. No correlation was found between the percentage of stenosis and venous dialysis pressure.

CONCLUSION We found a weak correlation between the degree of stenosis and blood pump flow rate, and no correlation between the percentage of stenosis and venous dialysis pressure.

CATEGORY: MYSIR 2018: INTERVENTIONAL RADIOLOGY (NON-NEUROLOGICAL)

MY002

Extended endovenous laser therapy of the long saphenous vein: a safe procedure that reduces the need for additional sclerotherapy

*Eric Chung¹, Basri Johan Jeet Abdullah¹, Chai Hong Yeong¹*¹Biomedical Imaging, University of Malaya, Malaysia

INTRODUCTION The objective of this study was to examine the viability and safety outcome of extended saphenous laser ablation for the treatment of varicose veins in our centre.

METHODS 24 patients, with a total of 41 limbs, who had elected for endovenous laser therapy (EVLT) were recruited over a period of three years. Preprocedural diagnosis of saphenojunction incompetence was made following Doppler examination. EVLT was performed on the distal great saphenous vein above the ankle as compared to the conventional technique of below the knee. Ablation was then executed following standard protocol. After the procedure, patients were instructed to put on compression stockings and allowed ambulation. Patients were finally discharged with painkillers and prophylactic

antibiotics. Surveys were conducted for pain, swelling, numbness and recurrence of varicosity at one-, three- and six-month follow-ups. Any complications were also documented.

RESULTS Technical success was 100%. Immediate postprocedural symptoms included pain (95%), numbness (75%) and swelling (53%), which tapered down to 46%, 58% and 12%, respectively, at the one-month follow-up. Only one patient (2/41 limbs) had residual swelling after three months. All patients who underwent EVLT showed no evidence of recurrent varicosity after six months.

CONCLUSION Extended EVLT of the saphenous vein proved to be a safe procedure with the benefit of perforator branch ablation reducing the need for additional sclerotherapy.

CATEGORY: MYSIR 2018: INTERVENTIONAL RADIOLOGY (NON-NEUROLOGICAL)

MY004

Selective hepatic arterial embolisation of the hepatic arteriobiliary fistula secondary to lupus vasculitis

*Kia Sing Tan¹, Benny Young²*¹Radiology, Sarawak General Hospital, ²Radiology, Borneo Medical Centre, Malaysia

In this report, we highlight hepatic arteriobiliary fistula as a rare complication of lupus vasculitis. The condition can be diagnosed via computed tomography mesenteric angiography (CTA) and treated via hepatic arterial embolisation. A 37-year-old woman with known systemic lupus erythematosus (SLE) presented with acute epigastric pain and melaena. She also had symptoms of anaemia with a low haemoglobin count and required transfusion. Emergency oesophago-gastroduodenoscopy revealed haemobilia. CTA showed gallbladder haematoma and arterial blush from the left hepatic artery. Digital subtraction angiography was subsequently performed. The left hepatic artery showed immediate contrast drainage into the common bile duct from the segment 4 branch, suggesting hepatic arteriobiliary

fistula. The artery is irregular in appearance, which suggested vasculitic changes. As the patient had no prior recent trauma or transhepatic procedure, the underlying SLE with vasculitis was the most likely cause of fistula formation. Selective embolisation was then performed using GELFOAM® and bleeding into the common duct was successfully controlled. The patient recovered without any serious sequelae. As she showed clinical improvement and a stable haemoglobin level, no follow-up imaging was done. Transcatheter embolisation is shown to be a quick and effective method to treat both traumatic and nontraumatic causes of hepatic arteriobiliary fistula. The source and cause of the haemorrhage can be identified, and haemostasis can be achieved in the same setting.

CATEGORY: MYSIR 2018: INTERVENTIONAL RADIOLOGY (NON-NEUROLOGICAL)

MY005

Selective salpingography and fallopian tube recanalisation: the University Malaya Medical Centre experience

*Man Chin Ham¹, Anushya Vijayananthan¹, Ouzreiah Nawawi¹, Kartini Rahmat¹, Chai Hong Yeong¹, Gnana Kumar Gnanasuntharam¹, Basri Johan Jeet Abdullah¹*¹University of Malaya Research Imaging Centre, University of Malaya, Malaysia

INTRODUCTION This study aimed to establish selective salpingography (SSG) and fallopian tube recanalisation (FTR) as treatment procedures for proximal tubal obstruction (PTO) at University Malaya Medical Centre (UMMC), Malaysia, by evaluating the effectiveness, complication, pain intensity and radiation dose.

METHODS We conducted a prospective study on nine patients aged 33.6 ± 3.17 years with the diagnosis of PTO by prior hysterosalpingography between October 2014 and December 2016 in UMMC. Fluoroscopic-guided FTR was performed by an intervention radiologist using a dedicated FTR set. Demographic data, recanalisation rate, postprocedure complications, pregnancy outcomes, pain score, radiation dose, and culture and sensitivity results were analysed. Patients were followed up for a period of 4–122 weeks.

RESULTS A total of 11 (four unilateral and seven bilateral) procedures, including two cases of repeat procedures, were performed. Out of 18

tubes, 14 were successfully recanalised, yielding a technical success rate per tube of 77.8% and a success rate per procedure of 90.9%. Post-FTR pregnancy rate was 50.0%; two pregnancies were achieved following repeat procedures. Two live births were reported. Seven patients experienced mild discomfort during the procedure. One case of tubal perforation occurred, but required no treatment. Mean fluoroscopic time was 8.6 ± 9.2 minutes. The range of dose area product recorded was 0.11–2.92 mGy m². Mean estimated effective dose was 2.63 ± 2.42 mSv. No significant bacterial growth was found.

CONCLUSION SSG and FTR are relatively safe and effective in treating highly selected patients diagnosed with PTO, as they have been shown to yield high technical success and pregnancy rates at a relatively low cost when compared to other invasive and costly reproductive treatments.

CATEGORY: MYSIR 2018: INTERVENTIONAL RADIOLOGY (NON-NEUROLOGICAL)

MY006

Common iliac vein stenting for the treatment of chronic lower limb swelling due to preferential drainage of the lower limb vein into the pelvic arteriovenous malformation

*Mohd Naim Mohd Yaakob¹, Nik Azuan Nik Ismail¹*¹Radiology, National University of Malaysia, Malaysia

We herein report a case of right common iliac vein occlusion with pelvic arteriovenous malformation (AVM), which was treated successfully via endovascular stenting. A 75-year-old man presented with diffuse right lower-limb swelling extending to the right lower abdomen, which had lasted for four months. Computed tomography angiography and diagnostic angiography of the lower limb showed evidence of short segment occlusion at the proximal right common iliac vein, with preferential flow into the collaterals and drainage into the AVM of the right hemipelvis, which extended to the right gluteal region. Common iliac venoplasty and stenting was performed, and we achieved successful

resolution of stenosis and saw a further marked clinical improvement of the swelling in the right leg. Subsequent follow-up revealed good outcome with no evidence of recurrence or post-stenting thrombosis. The initial presence of pelvic AVM may have perpetuated the iliac vein occlusion, which resulted in impaired venous drainage of the lower limb, and thus worsening of the swelling. A normal clinical pathway was established by means of balloon angioplasty, and a stent was placed to prolong the patency of the vein and avoid re-stenosis from preferential flow to the high-flow pelvic AVM.

CATEGORY: MYSIR 2018: INTERVENTIONAL RADIOLOGY (NON-NEUROLOGICAL)

MY007

Prostatic artery embolisation for acute urinary retention secondary to benign prostate hyperplasia

*Mohd Naim Mohd Yaakob¹, Nik Azuan Nik Ismail¹, Nur Yazmin Yaacob¹, Rozman Zakaria¹, Loo Wei Keong², Goh Eng Hong²*¹Radiology, ²Surgery, National University of Malaysia, Malaysia

INTRODUCTION This study aimed to assess the feasibility of prostatic artery embolisation (PAE) in treating patients with acute urinary retention (AUR) caused by benign prostate hyperplasia (BPH) who failed trial without catheter (TWOC).

METHODS Ten patients were recruited from the urology clinic and TWOC centre of Pusat Perubatan Universiti Kebangsaan Malaysia, Malaysia, to undergo PAE. Assessment was made using the International Prostate Symptom Score (IPSS), Quality of Life Scale (QoLS), International Index of Erectile Function (IIEF) Questionnaire, prostate-specific antigen test, uroflowmetry study of maximum flow rate (Qmax) and postvoid residual urine volume (PVR) in the bladder. Prostate volume was measured at baseline and at three-month follow-up using magnetic resonance (MR) imaging.

RESULTS Median age of the patients was 70.5 (IQR 66–79) years. Median duration of catheter *in situ* was 8 (IQR 4–18) months and

median BPH medication usage was 15 (IQR 1.75–48) weeks. Median prostate volume post embolisation was 62.25 (IQR 34.08–80.59) mL. Out of the ten patients, 9 (90.0%) achieved technical success, among whom 7 (77.8%) achieved clinical success. No procedure-related complications were observed. One of seven (14.3%) patients had a rate of AUR that required reinsertion of catheter within one month. Significant improvements to the IPSS and QoLS score were observed ($p < 0.003$ and $p < 0.030$, respectively). There were no significant changes to the patients' IIEF Questionnaire scores, which were measured again at follow-up. Qmax and PVR worsened in the first three months, but subsequently improved.

CONCLUSION PAE was found to be feasible, safe and efficient, and can be a treatment option for AUR caused by BPH.

CATEGORY: MYSIR 2018: INTERVENTIONAL RADIOLOGY (NON-NEUROLOGICAL)

MY008

A comparison of cone beam computed tomography with multislice computed tomography in the identification of common periprocedural intracranial pathologies

Nur Yazmin Yaacob¹, Izzatul Aini Mohamad Idris¹

¹*Diagnostic Imaging, Pusat Perubatan Universiti Kebangsaan Malaysia, Malaysia*

INTRODUCTION This study aimed to compare the sensitivity and specificity of cone beam computed tomography (CBCT) with those of multislice computed tomography (MSCT) in the detection of common periprocedural intracranial pathologies in patients undergoing angiography.

METHODS A total of 40 patients were included in this study. All patients underwent CBCT and MSCT during angiographic evaluation and neurointerventional procedures. Each intracranial event, encompassing haemorrhages, infarcts, hydrocephalus and external ventricular drains, was assessed via inter-observer ratings, and volumetric data was compared in both tomographic studies.

RESULTS Preliminary results showed high inter-observer correlation between the two imaging modalities in the detection of volumes of different intracranial pathologies. (Verified data was not available at the time of print but will be made accessible prior to the Conference.)

CONCLUSION CBCT is beneficial in the emergency management of periprocedural angiographic evaluation, as the detection of different intracranial events was found to be as reliable as in MSCT, with few exceptions. Technical limitations of CBCT are image artefacts, which may conceal paramount radiological findings. Further studies are thus warranted.

CATEGORY: MYSIR 2018: INTERVENTIONAL RADIOLOGY (NON-NEUROLOGICAL)

MY009

Comparing central line-associated bloodstream infection rate between tunnelled and cuffed peripherally inserted central catheters

Sze Yong Teoh¹, Anushya Vijayanathan¹, Ouzreiah Nawawi¹, Basri Johan Jeet Abdullah¹, Nur Adura Yaakup¹

¹*Biomedical and Diagnostic Imaging, University Malaya Medical Centre, Malaysia*

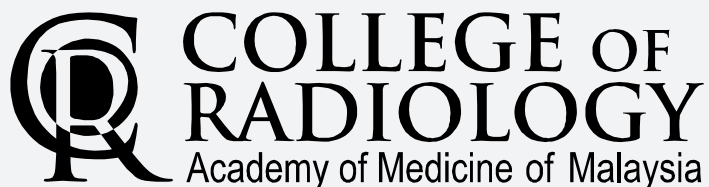
INTRODUCTION Peripherally inserted central catheters (PICCs) are now widely used, serving as alternatives to conventional central venous catheters (CVCs), in providing intermediate and long-term venous access in hospitals, especially for long-term antibiotic administrations, parenteral nutrition and chemotherapy. Complications related to PICCs include phlebitis, thrombosis, premature dislodgement and central line-associated bloodstream infection (CLABSI). Our goal was to determine the technique of PICCs insertion that can help to reduce the rate of CLABSI.

METHODS 50 patients with cuffed PICCs and 50 patients with non-cuffed (tunnelled) PICCs were randomly chosen and prospectively studied during an 18-month period. The tunnelled and cuffed catheters were placed by the same radiologist using a standardised technique. Patients were reviewed daily until any of these occurrences: PICC-related complication necessitating PICC removal; completion of therapy; death; or defined end-of-study date.

RESULTS Tunnelled PICCs were shown to cause a lower rate of CLABSI and a longer catheter dwell time compared to cuffed PICC (CLABSI: tunnelled PICC 6% vs. cuffed PICC 10%). Local infection rate of tunnelled PICCs was also proven to be lower compared to their counterparts. Cuffed PICCs, however, were superior at preventing catheter dislodgement.

CONCLUSION This study showed that tunnelled PICCs are more effective in increasing the catheter dwell time and reducing the rate of catheter removal caused by infection (local and CLABSI) compared to cuffed PICCs. In view of the ease of performing this procedure and the potential cost-saving benefits, we would recommend this technique in patients requiring PICCs, especially those who require a longer duration of use.

Co-organisers



Supported by



STROKE COUNCIL

Malaysian Society of Neurosciences (Persatuan Neurosain Malaysia)



Endorsed by

